Confined transverse-optical phonons in ultrathin CdTe/ZnTe superlattices

T. Fromherz
Institut für Halbleiterphysik, Johannes Kepler Universität, A-4040 Linz, Austria

F. Hauzenberger
Institut für Experimentalphysik, Johannes Kepler Universität, A-4040 Linz, Austria

W. Faschinger and M. Helm
Institut für Halbleiterphysik, Johannes Kepler Universität, A-4040 Linz, Austria

P. Juza and H. Sitter
Institut für Experimentalphysik, Johannes Kepler Universität, A-4040 Linz, Austria

G. Bauer
Institut für Halbleiterphysik, Johannes Kepler Universität, A-4040 Linz, Austria
(Received 29 May 1992)

We report far-infrared reflectivity measurements on short-period $(CdTe)_n/(ZnTe)_n$ ($n=2,3,4,5$) superlattices. The superlattices were grown by atomic-layer epitaxy on a thick ZnTe buffer deposited on [001]-oriented GaAs substrates. The frequencies of transverse-optical phonon modes confined in the CdTe layers decrease systematically with increasing number of monolayers, n, whereas the corresponding confined modes in the ZnTe layers do not depend on n. It is shown that these data allow one to map out the dispersion of the transverse-optical modes along the [001] direction in both CdTe and ZnTe. Furthermore, the strain distribution in the superlattices is analyzed.

I. INTRODUCTION

It is well known that layered semiconductor structures such as quantum wells and superlattices (SL's) lead not only to a modification of the electronic properties but, in a very similar way, to changes in the phonon properties. Even though these modifications are often not as obvious as in the electronic case, their study can lead to a better understanding of lattice vibrations in crystals.

The modification of the phonon spectrum in superlattices is crucially dependent on the capability of the phonons of one constituent material to propagate in the other material. Strongly overlapping phonon bands will lead to folded (but propagating) phonons very similar to electronic minibands in superlattices. This is mostly the case for acoustic phonons. For optical phonons, due to their small dispersion, either folded or strongly confined phonons can occur, depending on the overlap of the dispersions in the two constituent materials. For example, it has been demonstrated recently that optical phonons can even be confined in a single atomic layer of AlAs embedded in GaAs (since the phonon frequency of AlAs is sufficiently different from the GaAs phonon frequency).[1] On the other hand, $GaAs/Al_xGa_{1-x}As$ SL's will permit the existence of folded optical phonons, since GaAs-like phonons can propagate in both layers.

Extensive investigations have been performed on SL's based on the GaAs/Al(Ga)As system by Raman scattering[2–8] and recently also far-infrared reflectivity (FIR) measurements.[9] Wide-gap II-VI compound SL's, which have become of technological importance due to the advent of the blue-green semiconductor junction laser, have been studied much less. To our knowledge, so far Raman-scattering experiments have been performed on CdTe/ZnTe SL's,[10] $Cd_{1-x}Mn_xTe/Cd_{1-y}Mn_yTe$, and $ZnSe/Zn_{1-x}Mn_xSe$ SL's (Ref. 11) in order to get information on confined LO modes.

In the present paper, we use far-infrared reflectivity measurements of CdTe/ZnTe short-period superlattices to determine the frequency of TO phonons confined in the CdTe and ZnTe layers. The investigation of superlattices with different periods allows us to map out the TO-phonon dispersion in both material systems and obtain information about the strain distribution. It is shown, that both the ZnTe layers and the CdTe layers are highly strained.

II. EXPERIMENT

The $(CdTe)_n/(ZnTe)_n$ superlattices were grown by atomic-layer epitaxy (ALE) (Refs. 12 and 13) on an 800-nm-thick ZnTe buffer deposited on semi-insulting [001] GaAs substrates. The number of monolayers, n, was the same for both materials, and varied between 2 and 5. Therefore, for all superlattice samples investigated, pseudomorphic growth occurs for CdTe on ZnTe and vice versa, in agreement with a recent determination of the critical thickness in CdTe/ZnTe systems by Cibert *et al.*[14] For $n=6$, an onset of strain relaxation by misfit dislocations was observed.[14] By variation of the number of periods N, the total number of monolayers of each compound is kept constant ($N=900$) for all SL's. The

TABLE I. TO-phonon frequencies.

$(CdTe)_n(ZnTe)_n$	Periods	ω_{TO} (cm^{-1}) CdTe-SL	ZnTe SL	ZnTe buffer
$n=2$	450	151.7	174.1	180.7
$n=3$	300	150.3	173.6	181
$n=4$	225	149.1	173	180.7
$n=5$	180	148.6	173.8	180.7

detailed parameters of the samples are listed in Table I.

The structural properties of the samples were determined by high-resolution x-ray diffraction using Cu $K\alpha_1$ radiation and a four-crystal Bartels monochromator. The diffraction patterns in Fig. 1 show superlattice satellite peaks up to second order. By using ALE growth conditions, one is thus able to control the periods of the superlattice layers with high precision. This is shown in Fig. 1 by the excellent agreement of the ω values of the second-order satellite of the $(CdTe)_4/(ZnTe)_4$ superlattice and the first-order satellite of the $(CdTe)_2/(ZnTe)_2$ superlattice.

Far-infrared reflectivity measurements at nearly normal incidence were performed at $T=10$ K with a spectral resolution of 0.25 cm^{-1} using a Bruker IFS 113v Fourier-transform spectrometer. In order to avoid Fabry-Perot oscillations, the substrates were wedged at an angle of 5°.

III. RESULTS AND DISCUSSION

Experimental reflectivity spectra are shown in Fig. 2 for four short-period $(CdTe)_n/(ZnTe)_n$ SL's ($n=2,3,4,5$). In each spectrum, one can clearly distinguish three peaks: the most prominent peak at about 181 cm^{-1} is due to the interaction of the radiation with the TO-phonon mode of the ZnTe buffer layer. On the low-energy side of this peak a shoulder appears, which we attribute to the TO-phonon of the ZnTe layers in the superlattice. The frequencies of the ZnTe TO phonon in the superlattices are clearly shifted to lower values with respect to their frequency in the buffer, but they do not change significantly with the number of monolayers of ZnTe. The peak occurring at about 150 cm^{-1} is caused by the TO phonons in the CdTe layers of the SL's. The position of this peak clearly depends systematically on the number of CdTe monolayers. With increasing number of monolayers, the TO-mode frequency is shifted to lower values.

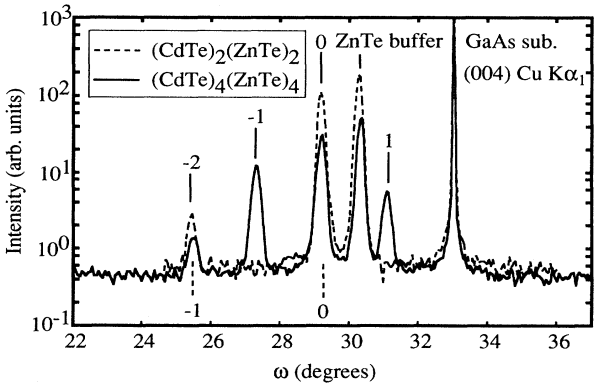

FIG. 1. Intensity of the (004) Bragg reflection vs the ω angle of a $(CdTe)_2/(ZnTe)_2$ SL (dashed curve) and a $(CdTe)_4/(ZnTe)_4$ (full curve) SL grown by ALE on a ZnTe buffer deposited on a [001] GaAs substrate. The order of the satellite peaks is indicated for both SL's.

In order to extract the phonon frequencies from the measured FIR spectra, the experimental data were fitted to a model that describes each layer (j) of the sample by a frequency-dependent dielectric function ε^j of the form

$$\varepsilon^j(\omega)=\varepsilon^j_\infty+\frac{\Delta\varepsilon^j\omega^2_{TO}}{\omega^j_{TO}{}^2-\omega^2-i\omega\Gamma^j}\ . \tag{1}$$

For CdTe and ZnTe $\Delta\varepsilon^j$, ω^j_{TO} and Γ^j are treated as fitting parameters. The values of ε^j_∞ are 7.1 and 6.7 for CdTe and ZnTe, respectively.[15] For the GaAs substrate, the well-established values for these parameters were used.[15]

By proper matching of the electric- and magnetic-field components at the interfaces and the use of the transfer-matrix method, one can simulate the reflection spectra.[16] The results of the fitting procedure are superimposed over the experimental data in Fig. 2. Since the difference between measured and calculated spectra is quite small, one can determine the phonon frequencies with an accuracy of ± 0.5 cm^{-1}. In Table I, the fitted TO-phonon frequencies are listed. The fitted values of $\Delta\varepsilon^j$, which determine the splitting of the LO- and TO-mode frequencies, lie in the range between 3.1 and 3.5 for the CdTe phonons, i.e., $\omega_{LO}=169.5-172.7$ cm^{-1}, which is realistic (the corresponding bulk value is 170 cm^{-1}).[15] For ZnTe the values of $\Delta\varepsilon^j$ range from 2.0 to 3.0, corresponding to $\omega_{LO}=206-218$ cm^1 (bulk value: 210 cm^{-1}). However, in contrast to the value of ω^j_{TO}, the fitted value of $\Delta\varepsilon^j$ depends very sensitively on the absolute reflectivity, which can vary slightly for different samples. The same is true for the broadening parameter Γ^j, for which the fitting

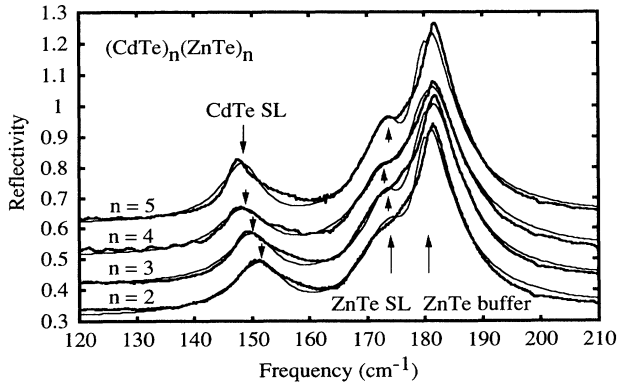

FIG. 2. Far-infrared reflectivity spectra of four $(CdTe)_n/(ZnTe)_n$ superlattices at nearly normal incidence. The bold lines represent the experimental data at $T=10$ K, the thin lines are the result of a fitting procedure described in the text. The arrows mark the TO-phonon frequencies obtained from the fits. For clarity, the reflectivity curves for the $n=3$, 4, and 5 SL's are shifted vertically in steps of 0.1.

procedure yields values between 5 and 7 cm^{-1}. Therefore, $\Delta\varepsilon^j$ and Γ^j cannot be determined with a high accuracy. This just reflects the fact that, for thin layers, LO-phonon frequencies cannot reliably be obtained through a measurement of the infrared reflectivity, but are better determined by Raman scattering.

We discuss now the effect of confinement on the phonon frequencies. In Fig. 3 the TO-phonon frequencies obtained from the fits for both ZnTe and CdTe are plotted versus the number of monolayers. As mentioned above, in contrast to the CdTe TO-phonon frequency, the frequency of the TO-phonon in the ZnTe layers does not vary with the layer thickness. This different behavior is interpreted as being caused by the bulk TO-phonon dispersion relations of ZnTe and CdTe, together with the effect of confinement. At nearly normal incidence, the radiation can only interact with TO phonons with a wave vector parallel to the growth direction of the superlattice (i.e., the [001] direction). As the bulk dispersion relations in the [001] direction of CdTe and ZnTe (Ref. 15) show, no TO-phonon mode can propagate in ZnTe at the TO-phonon frequency of CdTe (and vice versa). The large difference of the TO-phonon frequencies of about 35 cm^{-1} and the flatness of their bulk dispersion relations result in a strong confinement of the TO phonons in the individual superlattice layers. Therefore, no folded phonons, but rather strongly localized ones, occur. This situation is similar to the case of short-period GaAs/AlAs SL's, where only phonons with wave vector $k \approx m\pi/L$ can be excited in a layer with thickness L, where m is an integer. The exact dependence of the wave vector of confined modes on L and their order m depends on the choice of the model used (see, e.g., Refs. 5–7 for further discussion).

In our experiment, we only observed ground-state phonons ($m=1$). Figure 3 shows that the frequency of the confined TO phonons in CdTe is very sensitive to the thickness of the layers. Especially for small numbers n of monolayers, a thickness fluctuation of only one monolayer would lead to a significant broadening of the phonon peak in the reflection spectrum. Since the peak reflectivities of the CdTe TO modes for the four SL's are clearly different (Fig. 2), we conclude that the thickness fluctuations are extremely small (much less than one monolayer).

By varying the layer thickness in the SL's, one observes TO phonons at different wave vectors (see Fig. 2) and thus obtains information on their $\omega(k)$ dispersion relation. For CdTe, the TO-phonon dispersion relation determined by this optical method is plotted in Fig. 4, together with data obtained by inelastic-neutron-scattering experiments on bulk CdTe samples at $T=300$ K.[17] Since at low temperatures the TO-mode frequencies are shifted to higher values [in the Γ point from 140 cm^{-1} ($T=300$ K) (Ref. 17) to 144.7 cm^{-1} ($T=12$ K) (Ref. 18)], the offset between the two ordinate scales is partly due to the different temperatures of both types of experiments. The remaining offset of about 3 cm^{-1} is attributed to a shift caused by the biaxial compressive strain in all SL samples. The effect of strain is discussed in the next paragraph. The range of reduced wave vectors below 0.2 (in units of $2\pi/a$) was not accessible in the present experiment. For that purpose, $(CdTe)_n/(ZnTe)_n$ samples are needed with the number of monolayers $n \geq 6$. Then, the lattice mismatch is not only accommodated by strain, but also by misfit dislocations, since n is above the critical number of monolayers for pseudomorphic growth of CdTe on ZnTe.[14] The optically measured dispersion has an experimental error of 1 cm^{-1}, which is much less than the error bar on the neutron-scattering data. In addition,

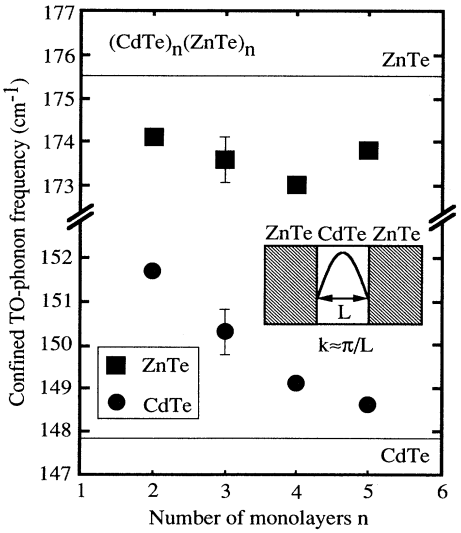

FIG. 3. Frequency of the TO modes confined to the CdTe layers (filled circles) and ZnTe layers (filled squares) as a function of the number of monolayers in the $(CdTe)_n/(ZnTe)_n$ SL's. The inset illustrates the connection between the wave vector of a strongly confined phonon in one layer and the confining length L. The horizontal lines mark the calculated phonon frequencies of strained bulk CdTe and ZnTe with strain-tensor components corresponding to a free-standing CdTe/ZnTe superlattice.

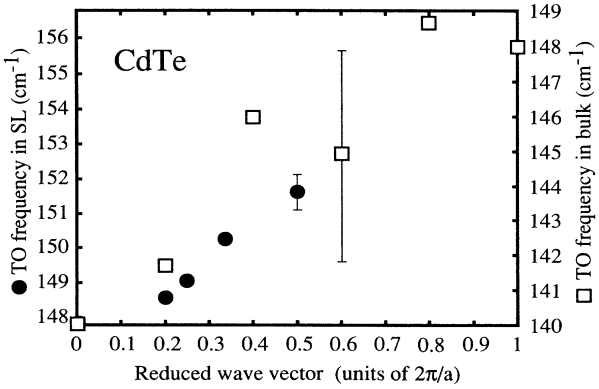

FIG. 4. TO-phonon frequency vs reduced wave vector for CdTe. The filled circles (left-hand vertical scale) are the result of the present work ($T=10$ K), whereas the open squares (right-hand vertical scale) are taken from inelastic-neutron scattering at 300 K (Ref. 17). The offset between the two different scales is due to the fact that the SL's are strained, and partly to the different temperatures of both experiments.

the excellent agreement of both dispersion relations confirms the model of confined TO phonons. Since the TO-phonon frequency of bulk CdTe increases with increasing wave vector, no linear-chain model can be used for analysis of the confined TO modes, contrary to the situation found in GaAs/AlAs SL's.[3] Also, no microscopic calculations based on an *ab initio* scheme have been published so far for short-period II-VI SL's, to our knowledge.

In bulk ZnTe, the TO-phonon frequency is nearly independent of the wave vector along the [001] direction.[15] For that reason, no shift of the confined ZnTe TO-phonon frequencies is observed in the reflectivity data of the different SL samples (Fig. 2). The measured value of the TO-phonon frequency in all ZnTe buffers (180.7 cm^{-1}) lies very close to the value for TO-phonons in bulk ZnTe at $T=12$ K (180 cm^{-1}).[18] Therefore, the difference between the ZnTe TO-phonon frequencies in the superlattices and in the buffer is attributed to the biaxial tensile strain in the ZnTe layers of the SL's. This strain is expected to be large because of the lattice mismatch of about 6.2% between ZnTe (6.10 Å) and CdTe (6.48 Å). The effects of strain on the phonon frequencies are discussed in the following.

In the zinc-blende lattice, long-range Coulomb forces split the TO- and LO-phonon modes at the Γ point. This splitting is essentially independent of the strain.[19] Consequently, the strain-induced splittings and frequency shifts are calculated first for the diamond lattice and then properly transferred to the zinc-blende structure. In a diamond lattice, the threefold degeneracy of the optical phonons in the Γ point of the Brillouin zone is lifted by the strain. A biaxial strain in the plane perpendicular to a [001] direction results in a change of the optical-phonon frequencies that can be considered as a sum of two contributions: (i) a shift ($\Delta\Omega_H$) caused by the hydrostatic part of the strain tensor and (ii) a splitting ($\Delta\Omega$) caused by the uniaxial part of the strain tensor in a onefold (Ω_S) and a twofold (Ω_D)-degenerate phonon frequency:[19,20]

$$\Omega_S=\omega_0+2\Delta\Omega_H-\tfrac{2}{3}\Delta\Omega \ , \tag{2}$$

$$\Omega_D=\omega_0+2\Delta\Omega_H+\tfrac{1}{3}\Delta\Omega \ . \tag{3}$$

In Eqs. (2) and (3), the hydrostatic shift $\Delta\Omega_H$ and the splitting term $\Delta\Omega$ are given by[19,20]

$$\Delta\Omega_H=-\gamma\omega_0\frac{S_{11}+2S_{12}}{S_{11}+S_{12}}\varepsilon_{xx} \ , \tag{4}$$

$$\Delta\Omega=a_s\omega_0\frac{S_{11}-S_{12}}{S_{11}+S_{12}}\varepsilon_{xx} \ , \tag{5}$$

where ω_0 is the phonon frequency without strain, γ is the mode Grüneisen parameter, a_s the shear deformation parameter, ε_{xx} the in-plane component of the strain tensor, and S_{11} and S_{12} are components of the elastic compliance tensor.

Equations (2) and (3) hold for zinc-blende structure if ω_0 is substituted by either ω^0_{LO} or ω^0_{TO} in an appropriate way. Since we observe in our experiment TO-phonon modes with wave vectors along the growth direction (i.e., the biaxial strain is in the plane perpendicular to it) the TO phonons remain twofold degenerate. Their frequency is given by Eq. (3):

$$\Omega_{TO}=\omega^0_{TO}+2\Delta\Omega_H+\tfrac{1}{3}\Delta\Omega \ . \tag{6}$$

The strain is determined by the in-plane lattice constant $a_\perp$ of the superlattice layers. We assume that the lattice mismatch between the CdTe and ZnTe layers in the SL's is accommodated by homogeneous strain not influenced by the ZnTe buffer. Further assuming that the superlattice is a free-standing one, $a_\perp$ is determined by the minimum of the elastic-energy density in the superlattice. Taking into account the difference in the elastic compliancies of CdTe and ZnTe, the in-plane lattice constant is given by

$$a_\perp=\frac{n_1a_1^2K_1+n_2a_2^2K_2}{n_1a_1K_1+n_2a_2K_2} \ , \tag{7}$$

where n_i is the number of monolayers, a_i the lattice constant of CdTe ($i=1$) and ZnTe ($i=2$). The constant K_i is defined by $K_i=(S_{11_i}+S_{12_i})^{-1}$.

The in-plane components of the strain tensor ε^i_{xx} are then obtained from

$$\varepsilon^i_{xx}=\frac{a_\perp-a_i}{a_i} \ . \tag{8}$$

In Table II, the parameters used for calculating the strain-induced shift of the TO-phonon frequencies are summarized. Among these, the values for a_s and γ are the ones with the highest uncertainty: to our knowledge, the value of γ has been experimentally determined for ZnTe,[21] whereas no experimental data exist for γ_{CdTe}. For both materials, a_s is not known. Theoretical arguments[21,22] indicate that both γ and a_s correlate with the ionicity of the compounds. Since CdTe, ZnTe, and ZnSe have approximately the same ionicity, the differences in the values of γ and a_s are expected to be small between these compounds. (As shown in Ref. 21, the values of γ_{ZnTe} and γ_{ZnSe} are the same within experimental error.) As an approximation, the values of γ and a_s are assumed to be identical for ZnTe and CdTe. Lacking experimental information on a_s for both CdTe and ZnTe, we use the corresponding value known only for ZnSe (Ref. 19) for the two other compounds.

Taking the parameters of Table II, the strain-induced

TABLE II. Parameters used for calculating the strain-induced shift of the TO-phonon frequency in CdTe and ZnTe (defined in the text).

	a (Å)	ω^0_{TO} (cm^{-1})	S_{11} (10^{-11} Pa^{-1})	S_{12} (10^{-11} Pa^{-1})	γ	a_s
CdTe	6.482[a]	144.7[b]	4.23[a]	−1.72[a]	1.7	0.6
ZnTe	6.104[a]	180[b]	2.40[a]	−0.87[a]	1.7[c]	0.6

[a]Reference 15.
[b]Reference 18.
[c]Reference 21.

shift of the ZnTe TO-phonon frequency is calculated by using Eqs. (4)–(8), and a decrease from the bulk value of 180 cm^{-1} (Ref. 18) to 175.5 cm^{-1} results. The CdTe TO frequency increases from 144.7 cm^{-1} (Ref. 18) to 147.8 cm^{-1} for these conditions. In Fig. 3, these strain-shifted values are marked by horizontal lines. Figure 3 shows that in the strained-layer SL's the ZnTe phonon frequencies deviate insignificantly from the calculated line. Since the values γ and a_s for ZnTe are not precisely known, the difference between the calculated value for the ZnTe TO-mode frequency of about 175.5 cm^{-1} and the observed values of about 174 cm^{-1} are unimportant. The agreement is even better for CdTe. Since for increasing number of monolayers the effects of confinement are reduced, the observed CdTe TO-mode frequencies approach the value calculated for strained bulk CdTe (indicated by the horizontal line at 147.7 cm^{-1} in Fig. 3).

Additional support for the assumption of a free-standing superlattice is obtained from earlier photoluminescence measurements on CdTe/ZnTe superlattices grown on $CdTe_{(1-x)}Zn_xTe$ buffers ($x \leq 0.5$).[23] These measurements have shown that independent of the Zn content of the buffer, the superlattices are in a free-standing configuration. In our case, the ZnTe buffer thickness is about 800 nm for all samples. Since the lattice mismatch between the GaAs and ZnTe is as large as 8%, the critical thickness for the pseudomorphic growth of ZnTe on GaAs is below four monolayers,[14] as determined by *in situ* reflection high-energy electron diffraction (RHEED). Therefore, the thickness of the ZnTe buffer is far beyond its critical thickness. Consequently, the buffer is completely relaxed, as evidenced by the measured TO-mode frequency and confirmed by x-ray-diffraction data.[12] For the superlattices, our calculations indicate a free-standing configuration, which is expected, since their total thicknesses are about 580 nm. Their average composition ($Cd_{0.5}Zn_{0.5}Te$) has a lattice mismatch of 3% with respect to the fully relaxed ZnTe buffer, which results in a critical thickness of about 13 monolayers.[14] Therefore, the total thickness of the CdTe/ZnTe stack (1800 monolayers) is again far above the critical one for pseudomorphic growth on the ZnTe buffer. Indeed, these results are confirmed by an analysis of symmetric (004) and asymmetric [(026), ($\bar{3}35$), ($\bar{3}\,\bar{1}\,\bar{5}$)] Bragg reflections on the $(CdTe)_3/(ZnTe)_3$ sample.[12]

IV. SUMMARY

The analysis of far-infrared reflectivity measurements of short-period CdTe/ZnTe superlattices provides accurate information on the effect of confinement and strain on the TO-phonon modes. The results demonstrate that the $(CdTe)_n/(ZnTe)_n$ SL's ($n=2,3,4,5$; number of periods: 450, 300, 225, 180) grown by ALE are free-standing. The localization of the TO phonons in the ultrathin CdTe layers with very small thickness fluctuations allowed us to obtain precise information on the dispersion of CdTe TO phonons along the [001] direction from $k=0$ to $k=\pi/a$ (halfway between Γ and X). Since for ZnTe, the TO modes show more or less no dispersion, the frequency of the confined modes in the ZnTe layers is independent of the ZnTe layer thickness within experimental uncertainty. Consequently, their frequency position was used for a strain analysis.

ACKNOWLEDGMENTS

This work was supported by the Jubiläumsfonds der Österreichischen Nationalbank under Project No. 4089 and by the Fonds zur Förderung der Wissenschaftlichen Forschung (P8446). We thank H. Krenn for helpful discussions concerning the simulation of far-infrared reflection spectra and A. Pesek and K. Lischka for their support with the x-ray measurements.

[1] H. Ono and T. Baba, Phys. Rev. B **44**, 12 908 (1991).
[2] B. Jusserand, D. Paquet, and A. Regreny, Phys. Rev. B **30**, 6245 (1984).
[3] C. Colvard, T. A. Gant, M. V. Klein, R. Merlin, R. Fischer, H. Morkoc, and A. C. Gossard, Phys. Rev. B **31**, 2080 (1985).
[4] A. K. Sood, J. Menéndez, M. Cardona, and K. Ploog, Phys. Rev. Lett. **54**, 2111 (1985).
[5] E. Molinari, A. Fasolino, and K. Kunc, Phys. Rev. Lett. **56**, 1751 (1986).
[6] B. Jusserand and D. Paquet, Phys. Rev. Lett. **56**, 1752 (1986).
[7] A. K. Sood, J. Menéndez, M. Cardona, and K. Ploog, Phys. Rev. Lett. **56**, 1753 (1986).
[8] S. Baroni, P. Giannozzi, and E. Molinari, Phys. Rev. B **41**, 3870 (1990).
[9] G. Scamarcio, L. Tapfer, W. König, A. Fischer, K. Ploog, E. Molinari, S. Baroni, P. Giannozzi, and S. de Gironcoli, Phys. Rev. B **43**, 14 754 (1991).
[10] J. Menéndez, A. Pinczuk, J. P. Valladares, R. D. Feldman, and R. F. Austin, Appl. Phys. Lett. **50**, 1101 (1987).
[11] E. K. Suh, D. U. Bartholomew, A. K. Ramdas, S. Rodriguez, S. Venugopalan, L. A. Kolodziejski, and R. L. Gunshor, Phys. Rev. B **36**, 4316 (1985).
[12] F. Hauzenberger, W. Faschinger, P. Juza, A. Pesek, K. Lischka and H. Sitter, Thin Solid Films (to be published).
[13] W. Faschinger and H. Sitter, J. Cryst. Growth **111**, 99 (1990).
[14] J. Cibert, R. André, C. Deshayes, G. Feuillet, P. H. Jouneau, Le Si Dang, R. Mallard, A. Nahmani, K. Saminadayr, and S. Tatarenko, Superlatt. Microstruct. **9**, 271 (1990).
[15] *Landolt-Börnstein Tables,* edited by O. Madelung and M. Schulz (Springer, Berlin, 1987), Vol. III/22a.
[16] B. Harbecke, Appl. Phys. B **39**, 165 (1986).
[17] J. M. Rowe, R. M. Nicklow, D. L. Price, and K. Zanio, Phys. Rev. B **10**, 671 (1974).
[18] D. J. Olego, P. M. Raccah, and J. P. Faurie, Phys. Rev. B **33**, 3819 (1986).
[19] F. Cerdeira, C. J. Buchenauer, F. H. Pollak, and M. Cardona, Phys. Rev. B **5**, 580 (1972).
[20] S. Venugopalan and A. K. Ramdas, Phys. Rev. B **8**, 717 (1973).
[21] S. S. Mitra, O. Brafman, W. B. Daniels, and R. K. Crawford, Phys. Rev. **186**, 942 (1969).
[22] D. N. Talwar, M. Vandevyver, K. Kunc, and M. Zigone, Phys. Rev. B **24**, 741 (1981).
[23] R. H. Miles, G. Y. Wu, M. B. Johnson, T. C. McGill, J. P. Faurie, and S. Sivananthan, Appl. Phys. Lett. **48**, 1383 (1986).